The 2014 World Congress on
Advances in Civil, Environmental, and Materials Research (ACEM14)
Busan, Korea, August 24-28, 2014

Design wind loads for open-type framed membrane structures

*Yuki Takadate[1),Eri Gavanski[2)and Yasushi Uematsu[3)

[1), 2), 3)] *Department of Architecture and Building Science, Tohoku University, Sendai 980-8579,Japan*
[1)] *takadate-y@hjogi.pln.archi.tohoku.ac.jp*

ABSTRACT

Wind force coefficients for designing open-type framed membrane structuresareproposed based on a wind tunnel experiment. Two cases of gable-wall opening are investigated; only one gable wall is open in a case, while both gable walls are open in the other case. For a comparative purpose, a closed-type model is also tested. Wind pressures are measuredsimultaneously at many points both on the external and internal surfaces of the model in a turbulent boundary layer. For discussing the design wind loads on the main wind force resisting systems, focus is on the bending moment involved in the windward column as the load effect. Furthermore, the peak wind force coefficients for cladding designare specified based on the distributions of the most critical positive and negative peak wind force coefficients irrespective of wind direction.

1. INTRODUCTUION

Open-type framed membrane structures are oftenused for temporary buildings and sports facilities (see Fig.1). Being light and flexible, such structures are vulnerable to wind actions. Furthermore, because both the external and internal surfaces are immersed in the flow, the resultant wind forces are more complicated than those on enclosed structures. Whereas a large database of knowledge exists for wind pressure distributions on enclosed buildings of various shapes, only a few studies have been made of the wind loading on open-type structures, probably due to difficulties in model making and wind pressure measurements. Indeed, the Notification No. 1454 of the Ministry of Construction, Japan (2000) specifies the internal pressure coefficient for structures with a large opening in the windward or leeward wall, which can be used for evaluating the wind forces by combining the external pressure coefficients. However, only a wind direction normal to the wall is considered in the specification. To the authors' best knowledge, few studies have been made of the wind loading onopen-type buildings as shown in Fig. 1.

[1)] Graduate Student
[2)]Assistant Professor
[3)] Professor

The present paper discusses the wind force coefficients for designing the main wind force resisting systems (structural systems) and cladding of open-type framed membrane structures, based on a wind tunnel experiment. In the experiment, wind pressures both on the external and internal surfaces are measured simultaneously to evaluate the net wind forces on the frames directly. For discussing the design wind force coefficients for the main wind force resisting systems,focus is on the bending moments involved in the windward column as the most important load effect. The LRC method and a conditional sampling technique are employed in order to consider the time-space correlation of wind forces, which provide the equivalent static wind loads. Based on the results for the most critical condition (i.e. frame location and wind direction), a simple model of the design wind force coefficient is proposed. Furthermore, the peak wind force coefficients, both positive and negative, for designing the cladding are proposed, based on the distributions of the most critical positive and negative peak wind force coefficients irrespective of wind direction.

It should be mentioned that the present paper is an extended version of our previous paper (Uematsu et al. 2013). A detailed discussion of the design wind force coefficients for the main wind force resisting systems is made. Furthermore, the peak wind force coefficients for cladding design are provided.

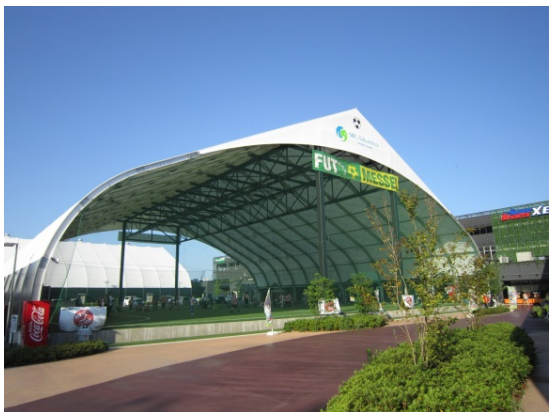

Fig. 1 An example of open-type structure

2. EXPERIMENTAL APPARATUS AND PROCEDURES

Wind-tunnel experiments are carried out in a turbulent boundary layer wind tunnel, which has a working section of 1.4m wide, 1.0m high and 6.5m long (Fig. 2). A turbulent boundary layer with a power law exponent of α = 0.21 for the mean wind speed profile is generatedon the wind tunnel floor. The profiles of the mean wind speed and turbulence intensity of the wind tunnel flow are shown in Fig. 3.

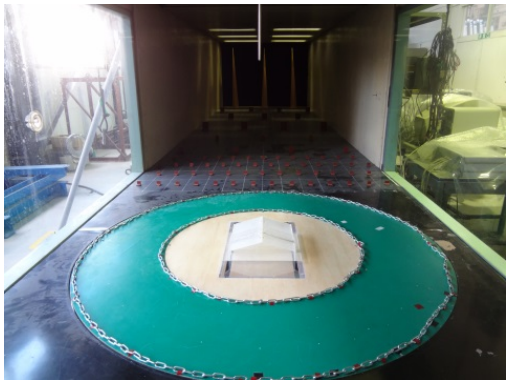

Fig. 2 Experimental model placed in the wind tunnel

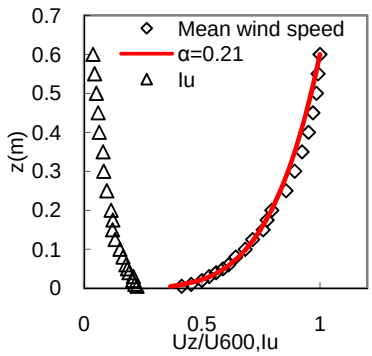

Fig. 3 Profiles of the mean wind speed and turbulence intensity of the wind tunnel flow

Fig. 4 shows the experimental model, which is a 1:200 scale model of typical framed membrane structures used for temporary buildings and sports facilities in Japan. It is assumed that the structure consists of planar frames constructed of H-section steel members, which are arranged in parallel and connected with one another by steel beams and braces. The experimental model consists of a sandwich structure of thin plastic sheets; the thickness is 4 mm. Sixteen pressure taps of 0.5 mm diameter are drilled along each line, 1-8, on each side of the model. Tapping locations are identical on the external and internal surfaces so that the pressure difference (net wind force) can be obtained directly. The pressure taps are connected to pressure transducers via a bronze tube of 0.5 mm ID and a PVC tube of 1.4 mm ID. The connections between the bronze and PVC tubes are all made beneath the wind tunnel floor. The total length of the tube is1m. The wind pressures at 32 taps along each line are measured simultaneously. The signals from the 32 pressure transducers are samples in parallel at a rate of 500 Hz on each channel for a period of approximately 12 sec (10 min in full scale, corresponding to the standard average time used for wind speed measurements in Japan). The measurement under the same condition is repeated 10 times.The statistics of the wind pressures and forces, such as the minimum peak pressure coefficients, are computed by applying ensemble average to the results of ten consecutive runs. The tubing effects are numerically compensated by using the gain and phase-shift characteristics of the pressure measuring system.

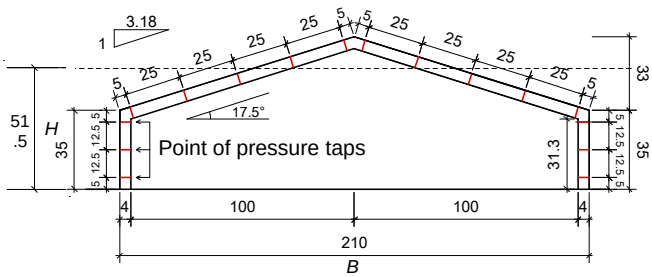

(a) Cross section (unit : mm)

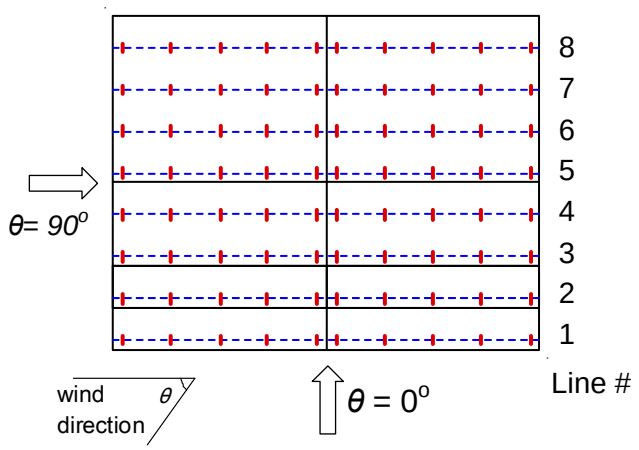

(b) Pressure tap layout and definition of wind direction

Fig. 4 Wind tunnel model

Three types of gable wall configurations, as shown in Fig. 5, are tested. Model 1 corresponds to the enclosed building, in which only the external pressures are measured. The wind direction θ is varied from 0 to 180° at a step of 15°(see Fig. 4(b)); θ = 0° represents a wind direction parallel to the ridge. Note that the windward gable wall is open when θ = 0° in Model 3.

The measurements are carried out at a mean wind velocity of $U_H \approx$ 8m/s at the mean roof height,H. The velocity scale,λ_V,is assumed 1/4, resulting in a time scale of λ_T=1/50, considering that the geometric scale is λ_L=1/200.

The wind pressure coefficient C_p is defined in terms of the velocity pressure q_H at the mean roof height H. The net wind force (pressure difference) coefficient C_f is defined as the difference between the external and internal pressure coefficients;hence, the direction of positive wind force coefficient isthe same as that of the external pressure coefficient.

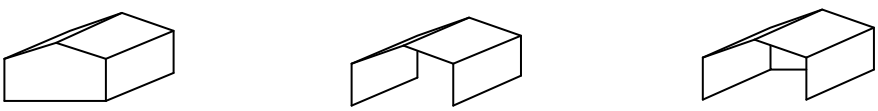

(a) Model 1 (closed-type) (b) Model 2 (open-type) (c) Model 3 (partially closed-type)

Fig. 5Gable wall configurations in the wind tunnel models

3. DISTRIBUTION OF MEAN WIND FORCE COEFFICIENTS

Fig.6 shows the $C_f$distributions on the three models for typical wind directions of θ = 0°, 15°, 45°, and 90°. Note that the internal pressureis assumed to be zero in Model 1; hence, the external pressure coefficientC_{pe}, coincides with the wind force coefficient C_f. From these results, the following features can be observed:

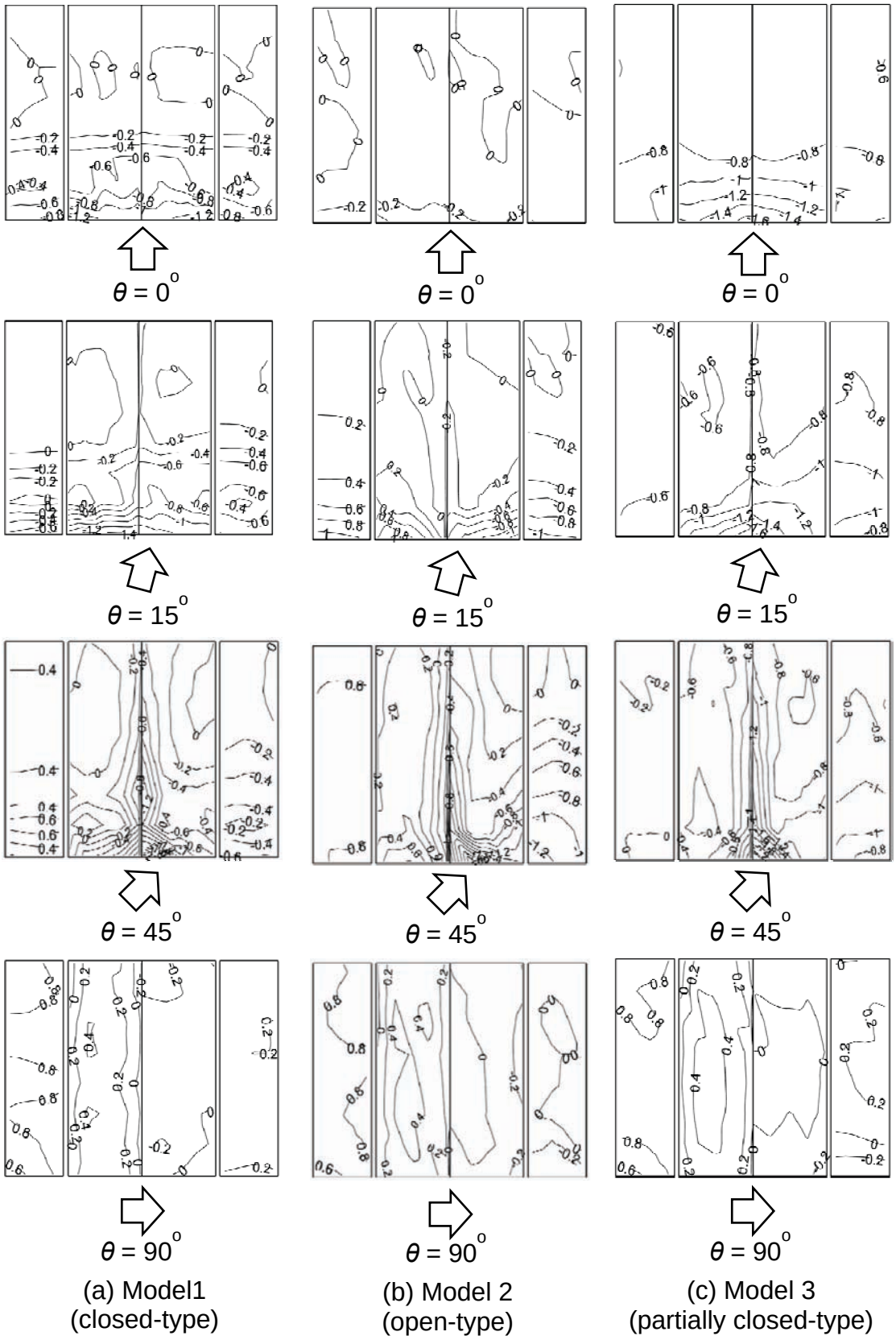

(a) Model1 (closed-type) (b) Model 2 (open-type) (c) Model 3 (partially closed-type)

Fig.6Distributions of the mean wind force coefficients for typical wind directions

(1) The $C_f$values on Model 2 for θ= 0° -45° are generally small in magnitude, compared with those on the other models. This feature is due to the flow inside the building in Model 2. In Model 3, on the other hand, the flow is stagnant, generating large positive internal pressures.
(2) Whenθ= 0°, the C_f distribution on Model 3 is quite similar in pattern to that on Model 1. The difference in the C_f value is approximately 0.4, indicating that the internal pressure coefficients on Model 3 are nearly equal to 0.4.
(3) The C_f distributions on the three models look similar to each other whenθ> 45°. It is interesting to note that the distributions on Models 2 and 3 are similar to each other when θ = 90°. Thais featureindicates that the distribution becomes less sensitive to the gable wall configuration with an increase inθ.
(4) In oblique winds, such as θ= 45°, large negative wind forces are induced in the windward area of the leeward roof, probably due to the generation of conical vortices. As a result, the C_f distribution in a cross section becomes asymmetric with respect to the ridge.

4. DESIGN WIND FORCE COEFFICIENTS FOR THE MAIN WIND FORCE RESISTING SYSTEMS

4.1 Load effect under consideration

For evaluating the design wind loads, the following assumptions are made:

(1) The frame is rigid enough to neglect the resonance effect. That is, only the back-ground component is taken into account.
(2) The frame is located along the lines of pressure measurements (Fig. 4). The same number is used both for the pressure measurement line and the frame.
(3) The member of frames is steel wide flange (H-294x200x8x12).
(4) The tributary width of Frame 1 is one half of that of the other frames.
(5) The column base is either pin-jointed or clamped to the footings.
(6) Focus is on the bending moment involved in the frame as the load effectfor discussing the design wind force coefficients.

Uematu et al. (2005) indicate that we can select the load effect to be considered in the load estimation, based on the results of a static analysis of the frame under mean wind loads for relatively small buildings where quasi-static response is predominant. Hence, we made such anstatic analysis for all frames and wind directions. The results indicate that we may focus on the bending moment at the knee and column base of the windward column for the pinned and clumped base frames, respectively. Therefore, the bending moments at these points are considered hereafter.

The time history of bending moment $M(t)$ may be given by the following equation:

$$M(t) = q_H \sum_j \alpha_j C_{pj}(t) A_j \qquad (1)$$

where α_j, C_{pj}(t) and A_j represent the influence coefficient, wind pressure coefficient and tributary area at Point j, respectively. Note that the influence coefficient α_j refers to the response to the unit force applied to Point j. The bending moment $M(t)$ is reduced to a non-dimensional value $M^*(t)$ as follows:

$$M^*(t) = \frac{M(t)}{q_H HBd} \tag{2}$$

where$B$ is the span of the frame (see Fig. 4); and $d$is the tributary width of each frame

Using the time history of wind pressure coefficients obtained from the wind tunnel experiment, the time history of non-dimensional bending moment $M^*(t)$ at the knee or base of the windward column is computed, from which the mean and the maximum value of the non-dimensional bending moment, $\overline{M}^*$ and$\widehat{M}^*$, are obtained. Fig. 7 shows the variation of $\widehat{M}^*$withθ for some frames. As might be expected from the distribution of the mean wind force coefficients (Fig. 6),oblique winds (θ =15° - 45° or θ =135° - 165°) produce the largest value of $\widehat{M}^*$ to a frame located near the windward gable end.It is thought that the largest value of $\widehat{M}^*$ is induced by conical vortices generated by the flow separation at the windward gable end. Regarding the central frame (Frame 5) of Model 1, the largest value of $\widehat{M}^*$ occurs at a wind direction ranging from 60° to 120°. This is the reason why the wind force coefficient is specified for such a wind direction in the code. However, the values of $\widehat{M}^*$ for the frames located near the gable end in oblique winds are much larger than that for the central frame in a wind normal to the ridge. For Model 3, a wind direction ofθ ≈15° produces the largest $\widehat{M}^*$ on Frame 2. These results indicate that the design wind force coefficient should be specified based on the results for oblique winds.

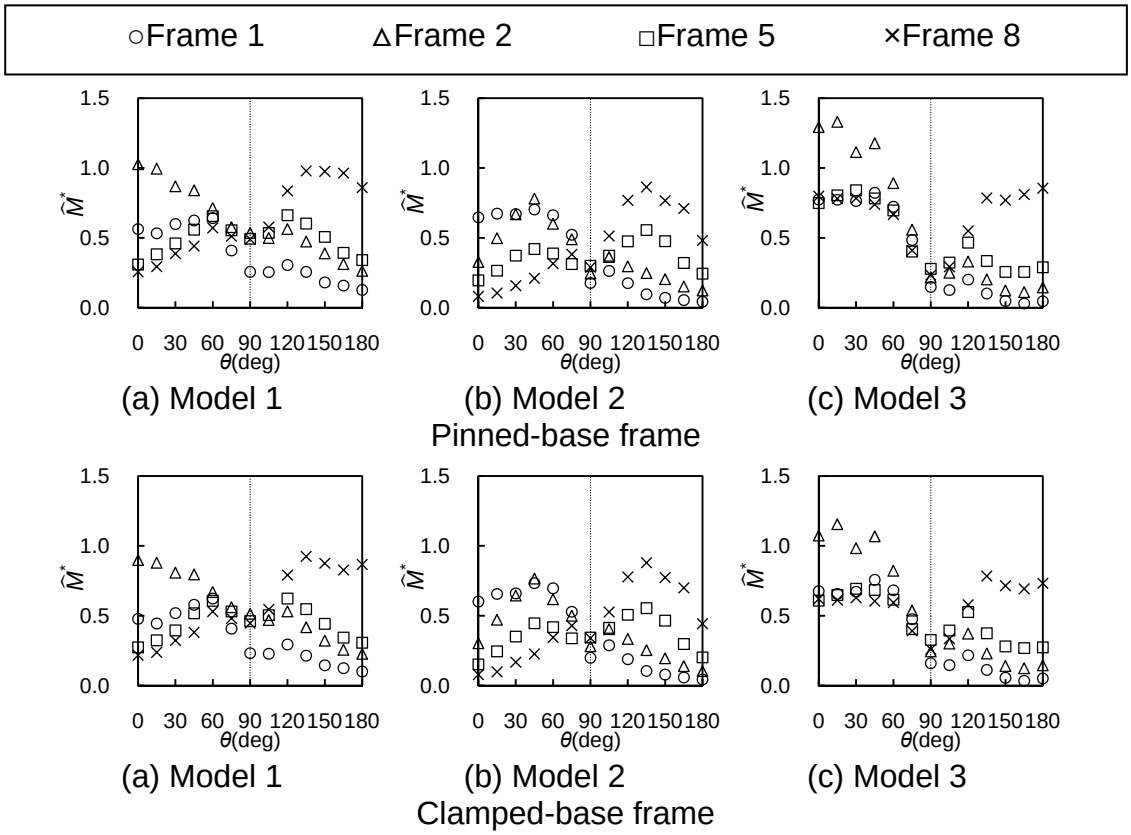

Fig. 7 The maximum load effects in typical frames for various wind directions

Table 1 show the frame number and wind direction where the maximum non-dimensional bending moment $\widehat{M}^*$ occurs. Thegust effect factor in the tableis calculated asfollows:

$$G_f = \frac{\hat{M}^*}{\overline{M}^*} \tag{3}$$

where $\widehat{M}^*$and $\overline{M}^*$ arerespectively the non-dimensional maximumpeak and the mean bendingmomentobtained from the time history of wind pressures.The value of G_f is larger in Model 3 than in Models1 and 2. Thisfeature implies that more severe load is applied to Model 3 than to the other cases.

Table1 The critical condition providing themaximum $\widehat{M}^*$ and the corresponding gust effect factor$G_f$for each model

	Pinned-base frame			Clamped-base frame		
Model	Frame number	θ(deg)	G_f	Frame number	θ(deg)	G_f
1	8	165	2.4	8	135	2.2
2	8	135	2.4	8	135	2.4
3	2	15	2.9	2	15	3.0

4.2 Distribution of the equivalent static wind force coefficients

For discussing the design wind force coefficients, the following three methods are employed in the present paper.

(1) Load Response Correlation (LRC) method:

This method proposed by Kasperski (1992) provides the equivalent static wind pressure coefficient C_{p_LRC} producing the maximum load effect, which is represented by the following equation:

$$C_{p\_\mathrm{LRC}} = \overline{C}_p \pm g_r C'_p \rho_{rp} \tag{4}$$

where $\overline{C_p}$is the mean wind pressure coefficient;g_r is the peak factor calculated form the time history of the load effect;$C_p^{'}$ is the RMS fluctuating pressure coefficient; and ρ_{rp} is the correlation coefficient between C_p and the load effect. When considering the wind force coefficient, we may use the wind force coefficient C_f instead of the wind pressure coefficient C_p in Eq. (4).

(2) Conditional sampling technique:

This method provides the instantaneous distribution of wind pressure (or force) coefficient, C_{p_cond} or C_{f_cond}, at an instant when the maximum peak value of the load effect occurs during a period of 10 min in full scale.

(3) Gust effect factor approach:

The design wind force coefficient is given by the product of the mean wind pressure (or force) coefficient and the gust effect factor G_f.

Fig.8 shows the distributions of wind force coefficients obtained from the above mentioned three methods for the most critical condition (Table 1), in which the distribution of the mean wind force coefficient is also plotted. Note that the abscissa of the figure is the distance s from the windward base along the frame normalized by the maximum value s_{max} (total length of the frame). For Model 1 (enclosed model), the internal pressure is assumed to bezero; therefore the external pressure coefficient

coincides with the wind force coefficient.It is clear that the distributions of C_{f_LRC} and C_{f_cond} are generally in good agreement with each other. The results of the gust effect factor approach, C_{f_Gust}, are generally large in magnitude than those of the LRC method and conditional sampling technique. This feature implies that both C_{f_LRC} and C_{f_cond} are affected by the vortices generated from the flow separation at the windward gable end and ridge as well as by the approaching turbulence. From these results, it may be concluded that the LRC method provides an appropriate estimation of the design wind force coefficients.

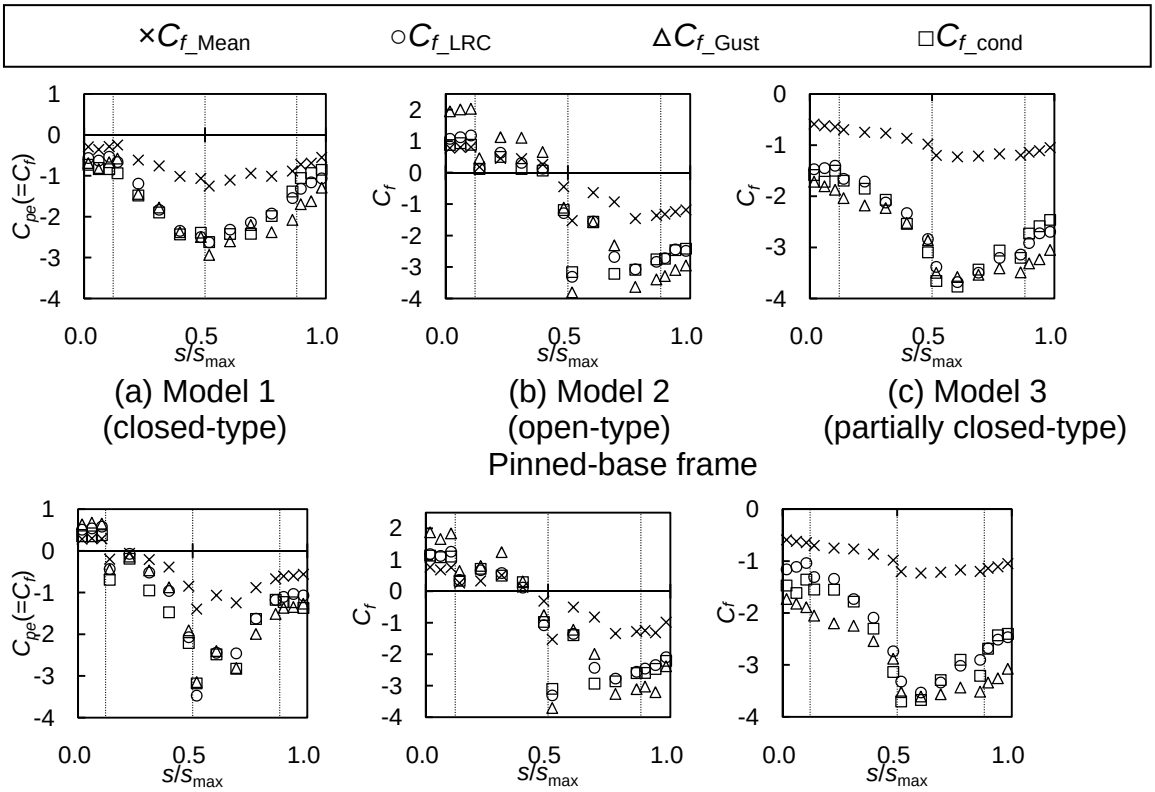

(a) Model 1 (closed-type) (b) Model 2 (open-type) (c) Model 3 (partially closed-type)

Pinned-base frame

(a) Model 1 (closed-type) (b) Model 2 (open-type) (c) Model 3 (partially closed-type)

Clamped-base frame

Fig.8Distribution of the structural wind force coefficients obtained from various methods

4.3 Simple model of the wind force coefficients

The previous section indicates that the LRC method provides a reasonable estimation of the equivalent static wind force coefficient for designing the mean wind force resisting systems. Then, a simplified model of the design wind force coefficient is specified as follows:

Step 1: The distribution of C_{f_LRC} on each wall or roof is spatially averaged. The averaged values are denoted as $\widehat{C}_{f\mathrm{WU}}$, $\widehat{C}_{f\mathrm{RU}}$, $\widehat{C}_{f\mathrm{RL}}$and $\widehat{C}_{f\mathrm{WL}}$ for the windward wall, windward roof, leeward roof and leeward wall, respectively.

Step 2: The load effect under consideration$\widehat{M}_{\mathrm{model}}$ (bending moment at the knee or base) is computed using the averaged wind force coefficient obtained in Step 1, and compared

with the maximum peak value $\widehat{M}_{\mathrm{TH}}$ obtained from the time history analysis using the wind tunnel data of wind pressure time history. Then, the ratio R of $\widehat{M}_{\mathrm{TH}}$to $\widehat{M}_{\mathrm{model}}$ is computed. The values of R are summarized in Table 2.

Step 3: The design wind force coefficients $C_{f\mathrm{WU}}$, $C_{f\mathrm{RU}}$, $C_{f\mathrm{RL}}$ and $C_{f\mathrm{WL}}$ for the four zones are provided as follows:

$$C_{f\mathrm{WU}} = \frac{\hat{C}_{f\mathrm{WU}} \cdot R}{G_f},\ C_{f\mathrm{RU}} = \frac{\hat{C}_{f\mathrm{RU}} \cdot R}{G_f},\ C_{f\mathrm{RL}} = \frac{\hat{C}_{f\mathrm{RL}} \cdot R}{G_f},\ C_{f\mathrm{WL}} = \frac{\hat{C}_{f\mathrm{WL}} \cdot R}{G_f} \qquad \text{(4a-d)}$$

The results for these wind force coefficients are summarized in Table 3. It is found that the distribution of the wind force coefficient obtained here is quite different from that specified in the building codes and the AIJ Recommendations for Loads on Buildings (2004). This is because the wind force coefficients proposed here are determined from the distribution of wind forces at a cross-section near the windward gable end in an oblique wind, while those specified in the building codes etc. are determined from the distribution at the central cross section in a wind normal to the ridge. The present paper clearly indicates that the largest load effect is induced in the frame located near the windward gable end in an oblique wind for all models. Therefore, the design wind force coefficient should be specified by considering such a critical condition, provided that the structure is consists of the same planar frames.

Table 2 Ratio of $\widehat{M}_{\mathrm{TH}}$ to $\widehat{M}_{\mathrm{model}}$ ($\widehat{M}_{\mathrm{TH}}$: Maximum peak bending moment obtained from time-history analysis)

	Model 1	Model 2	Model 3
Pinned-base frame	1.16	1.05	1.06
Clamped-base frame	1.25	1.10	1.11

Table3Design wind force coefficients for the main wind force resisting systems

	Pinned-base frame				Clamped-base frame			
Model	$C_{f\mathrm{WU}}$ ($C_{pe\mathrm{WU}}$)	$C_{f\mathrm{RU}}$ ($C_{pe\mathrm{RU}}$)	$C_{f\mathrm{RL}}$ ($C_{pe\mathrm{RL}}$)	$C_{f\mathrm{WL}}$ ($C_{pe\mathrm{WL}}$)	$C_{f\mathrm{WU}}$ ($C_{pe\mathrm{WU}}$)	$C_{f\mathrm{RU}}$ ($C_{pe\mathrm{RU}}$)	$C_{f\mathrm{RL}}$ ($C_{pe\mathrm{RL}}$)	$C_{f\mathrm{WL}}$ ($C_{pe\mathrm{WL}}$)
1	-0.28	-0.84	-1.03	-0.57	0.30	-0.40	-1.29	-0.61
2	0.50	0.04	-1.15	-1.12	0.57	0.13	-1.05	-1.02
3	-0.52	-0.77	-1.36	-1.01	-0.41	-0.67	-1.20	-0.95

In the above discussion, we considered two types of structures, i.e. pinned-base and clamped-base frames, and proposed models of wind force coefficients for these structures. In practice, however, the column seems to be elastically supported at the base in many cases. In such a case, a question arises; which model should be used in practice? In order to investigate this subject we made the following two analyses.

Analysis I: We computed the load effects, $M_{\mathrm{pin\_pin}}$ and $M_{\mathrm{pin\_clamped}}$, induced in the pinned-base frame when the frame is subjected to the wind loads obtained from the wind force coefficients for pinned-base and clamped-base frames, respectively. It is found that the ratio of $M_{\mathrm{pin\_clamped}}$ to $M_{\mathrm{pin\_pin}}$ ranges from 0.81 to 0.95.

Analysis II: Similarly, we computed the load effects, $M_{\mathrm{clamped\_pin}}$ and $M_{\mathrm{clamped\_clamped}}$, induced in the clamped-base frame when the frame is subjected to the wind loads

obtained from the wind force coefficients for pinned-base and clamped-base frames, respectively. It is found that the ratio ranges from 1.04 to 1.21.

These results indicate that the model of wind force coefficients for the clamped-base frame provides somewhat conservative estimation of the load effect. Therefore, this model seems appropriate for practical design.

5. PEAK WIND FORCE COEFFICIENTS FOR CLADDING DESIGN

5.1 Most critical positive and negative wind force coefficients

Fig. 9 shows the distributions of the most critical positive and negative peak wind force coefficients, represented by $\widehat{C}_f$, irrespective of wind direction. Note that a moving average with an averaging time of 0.2 sec in full scale is applied to the time history of the wind force coefficients and the positive and negative peak values during a period of 10 min in full scale are obtained. The following features may be detected from these figures:

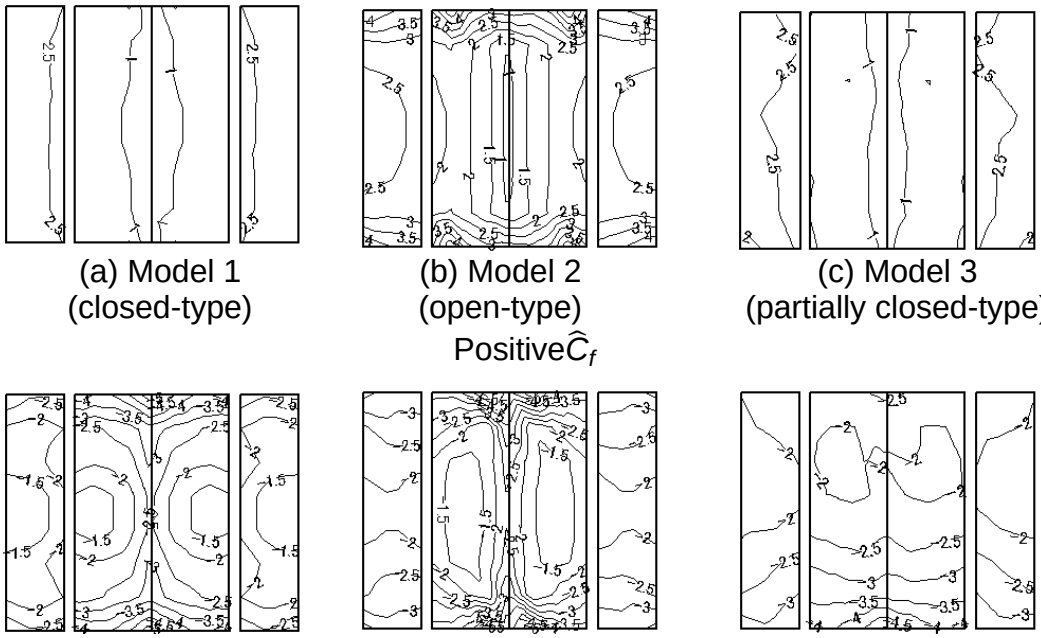

(a) Model 1 (closed-type) (b) Model 2 (open-type) (c) Model 3 (partially closed-type)

Positive $\widehat{C}_f$

(a) Model 1 (closed-type) (b) Model 2 (open-type) (c) Model 3 (partially closed-type)

Negative $\widehat{C}_f$

Fig.9 Distribution of the most critical positive and negative wind force coefficient irrespective wind direction

(1) The distributions of $\widehat{C}_f$, both positive and negative, on Models 1 and 3 look similar to each other. The magnitude of the negative $\widehat{C}_f$ values on Model 3 is larger than that those on Model 1. This is due to the effect of positive internal pressure in Model 3. Large negative $\widehat{C}_f$ values are induced along the gable ends, probably due to the vortex generation.

(2) Large negative $\widehat{C}_f$ values are also induced in the area near the gable end of Model 2. The magnitude is much larger than that on Models 1 and 3.
(3) The positive $\widehat{C}_f$ values on the roofs of Model 2 are generally larger than those on the other models. This is also due to the effect of internal pressure.

5.2 Peak wind force coefficients for cladding design

Based on the distributions of the most critical positive and negative wind force coefficients irrespective of wind direction (Fig. 9), the positive and negative peak wind force coefficients for designing the cladding and components are specified. Note that the positive and negative external pressure coefficients are provided for Model 1, which is combined with the internal pressure coefficient; the internal pressure coefficient is out of the scope of the present paper.

Fig. 10 shows the zoning of the peak wind force coefficients. The roof and wall are divided into several zones, and the positive and negative values are specified as shown in Tables 4 and 5. The zoning is the same as that used in the AIJ Recommendations for Loads on Buildings (2004), except for the positive wind force coefficient on Model 2.

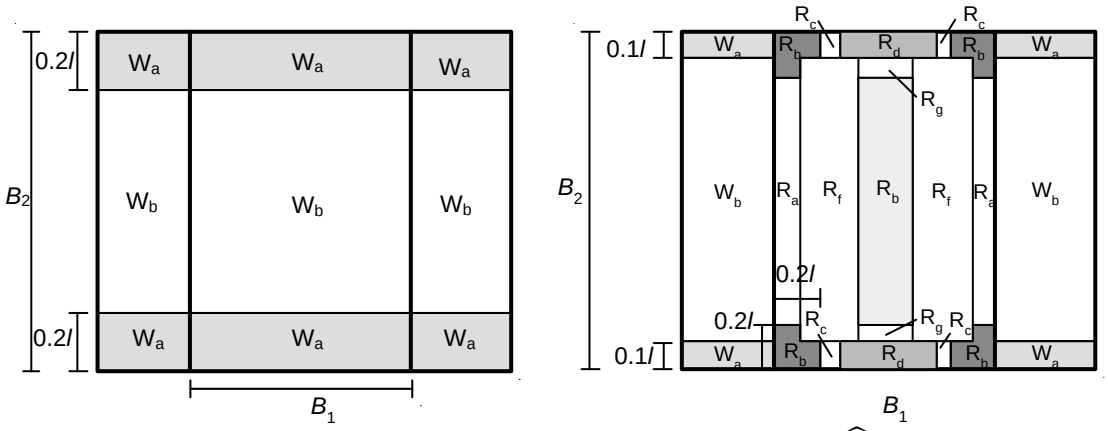

(a) Positive $\widehat{C}_f$ for Model 2 (b) Negative $\widehat{C}_f$ for Model 1-3

$l = \max(B_1, B_2, 4H)H$: mean roof height

Fig.10 Zoning for the peak wind force coefficients

Table 4Positive peak wind force (pressure) coefficients for cladding design

	W_a	W_b	R_a	R_b
Model 1	2.0	2.0	1.2	1.2
Model 2	3.5	2.5	3.0	2.0
Model 3	2.5	2.5	1.0	1.0
AIJ(2004)	2.0	2.0	0.1	0.1

Table 5 Negative peak wind force (pressure) coefficients for cladding design

	W_a	W_b	R_a	R_b	R_c	R_d	R_e	R_f	R_g
Model 1	-2.4	-1.8	-1.8	-3.0	-3.5	-4.0	-2.8	-2.0	-3.5
Model 2	-3.2	-2.2	-1.8	-3.2	-4.0	-4.5	-2.2	-1.5	-3.5
Model 3	-3.2	-2.2	-2.5	-3.5	-4.0	-4.2	-2.5	-2.4	-3.0
AIJ(2004)	-3.0	-2.4	-2.7	-3.8	-3.2	-4.9	-3.0	-2.5	-3.8

In the present study, the roof and wall are divided into two zones for the positive peak wind force coefficients on Model 2, because relatively large positive wind force coefficients are induced in the areas near the gable ends for Model 2. This feature is due to the effect of internal pressures in oblique winds. The value of the positive peak wind pressure coefficient for Model 1 is quite different from that specified in the AIJ Recommendations.According to the AIJ Recommendations, the positive peak wind pressure coefficientsfor roof zonesareprovided by Eqs.(5) and (6).

$$\hat{C}_{pe} = C_{pe}\left(1 + 7I_H\right) \tag{5}$$

$$C_{pe} = 0.014\left(\theta - 15\right) \tag{6}$$

where$\hat{C}_{pe}$, C_{pe}, I_H, and θrepresent the positive peak wind force coefficient, the positive external wind pressure coefficient,turbulence intensity at the mean roof height $H$and pitch angle of the gable roof, respectively.In the present model, the roof pitch is 17.5^o (see Fig. 4(a)), and the external wind pressure coefficient is estimated to be a small value,providing very small positive peak wind pressure coefficients.

The values of the negative peak pressure coefficients for Model 1 are somewhat smaller in magnitude than those specified in the AIJ Recommendations. This may be due to a fact that the AIJ Recommendations provide some conservative values considering a range of building geometry such as roof pitch and eaves height. It is interesting to note that the values of the negative peak wind force coefficients for Models 2 and 3 are not so different from each other.

6. CONCLUDING REMARKS

The wind force coefficients for designing the main force resisting systems and the peak wind force coefficients for cladding design were discussed.

Focus was on the bending moments at the base and knee of the windward column for the clamped-base and pinned-base frames respectively, as the most important load effects for discussing the design wind force coefficients for the main wind force resisting systems. First, we detected the most critical condition (frame location and wind direction) that provided the largest load effect. Actually, the largest load effect was induced for a frame located near the gable end in an oblique wind.Next, the equivalent static wind force coefficients were obtained by using the LRC method for the critical condition. Based on the results, a model of the design wind force coefficients is proposed by simplifying the distribution of the equivalent static wind force coefficients.

The most critical positive and negative wind force coefficients irrespective of wind direction were obtained. Based on the distributions of such wind force coefficients, the positive and negative peak wind force coefficients for cladding design were proposed. In

practice, the roofs and walls were divided into several zones, most of which were based on the AIJ Recommendations for Loads on Buildings (2004), and the positive and negative peak wind force coefficients were specified for these zones.

ACKNOWLEDGEMENT

A part of the present study is financially supported by Nohmura Foundation for Membrane Structure's Technology. Thanks are also due to Dr. Fumiyoshi Takeda, Taiyo Kogyo Corporation, for valuable discussion.

REFERENCES

Architectural Institute of Japan (AIJ).(2004). " Recommendations for Loads on Buildings", Tokyo, Japan.

Kasperski, M. (1992). Extreme wind load distributions for linear and nonlinear design. *Engineering Structures*, *14*(1), 27-34.

Uematsu, Y., Orimo, T., Watanabe, S., Kitamura, S. and Iwaya, M. (2005) "Wind loads on a steel greenhouse with a wing-like cross section"*Proceeding of the Fourth European & African Conference on Wind Engineering*, Prague, Czech Republic, 11-15 July, 2005, Paper #101.

Uematsu, Y., Takadate, Y. and Gavanski, E. (2013), "Design wind loads for frame-type membrane structure with various gable-end configurations,"*Research Reports on Membrane Structures 2013,* The Membrane Structures Association of Japan, No.27,15-22.(in Japanese)